Journal of Nuclear Materials 385 (2009) 449–455

Contents lists available at ScienceDirect

Journal of Nuclear Materials

journal homepage: www.elsevier.com/locate/jnucmat

Uranium–molybdenum nuclear fuel plates behaviour under heavy ion irradiation: An X-ray diffraction analysis

H. Palancher [a,*], N. Wieschalla [b], P. Martin [a], R. Tucoulou [c], C. Sabathier [a], W. Petry [b], J.-F. Berar [d], C. Valot [a], S. Dubois [a]

[a] CEA, DEN, DEC, F-13108 St. Paul Lez Durance Cedex, France
[b] Forschungsneutronenquelle Heinz Maier-Leibnitz (FRM II), Technische Universität München, D-85747 Garching bei München, Germany
[c] ID18F/ID22, ESRF, 6, rue J. Horowitz, 38043 Grenoble Cedex, France
[d] CRG/D2Am, ESRF, 6, rue J. Horowitz, 38043 Grenoble Cedex, France

ARTICLE INFO

PACS:
81.05.Bx
61.05.cp
61.72.U–
61.80.Jh
61.82.Bg
68.37.Hk

ABSTRACT

Heavy ion irradiation has been proposed for discriminating UMo/Al specimens which are good candidates for research reactor fuels. Two UMo/Al dispersed fuels (U–7 wt%Mo/Al and U–10 wt%Mo/Al) have been irradiated with a 80 MeV ^{127}I beam up to an ion fluence of 2×10^{17} cm^{-2}. Microscopy and mainly X-ray diffraction using large and micrometer sized beams have enabled to characterize the grown interaction layer: UAl_3 appears to be the only produced crystallized phase. The presence of an amorphous additional phase can however not be excluded. These results are in good agreement with characterizations performed on in-pile irradiated fuels and encourage new studies with heavy ion irradiation.

1. Introduction

A worldwide program encourages the development of low ^{235}U enriched fuels in order to convert research reactors cores (material test reactors, neutron sources, etc.) currently working with highly enriched (up to 93%) U_3Si_2 or UAl_x fuels. For the most powerful cores, high density UMo alloys appear to be the only fuel material that could enable their conversion without decreasing reactor performance.

UMo fuel elements for research reactors are usually rods or plates. In the latter concept, fissile materials can be either monolithic or dispersed (small particles in an Al matrix). In both cases, it is then pressed between Al sheets, used as cladding.

UMo fuel plates' behaviour under irradiation is currently not satisfactory because of the growth of a thick interaction layer at the UMo/Al interfaces [1–3]. Recent crystallographic investigations have shown that:

- At low temperatures (characteristic for fuel plate irradiation), this interaction layer appears to be amorphous. This has been shown using electron diffraction by only probing this interaction layer [4].
- At more elevated temperatures (typical for fuel rods irradiation), neutron diffraction indicates that the components of this interaction layer are crystalline (with mainly the UAl_3 crystallographic structure) [5,6]. In this case, influence of the burn-up has also been proved.

UMo fuel development is worldwide now essentially geared towards stabilizing and minimizing (or avoiding) this interaction zone. To overcome the difficulties inherent in the analysis of the in-pile irradiated samples, out-of-pile studies have to be performed. Extensive work has already been presented on UMo/Al interaction grown by thermal annealing [7–9]. This method is used to optimise fuel fabrication conditions.

To be representative of fuel plate in-pile irradiation conditions, annealing temperatures should be limited to a maximum of about 473 K or even lower. However, these low temperatures would imply very long annealing durations. Moreover, it is doubtful the extent to which thermal diffusion is able to simulate irradiation enhanced diffusion. Therefore, new tools have to be developed for evaluating nuclear fuels.

Heavy ion irradiation must be considered since it mimics fission fragment damages into the fuel: phenomena occurring during in-pile irradiation are better simulated. This method coupled or not with neutron irradiation has given some information to explain the unacceptable in-pile behaviour of U_3Si fuel [10,11].

* Corresponding author. Tel.: +33 442 257 555; fax: +33 442 253 285.
E-mail address: herve.palancher@cea.fr (H. Palancher).

0022-3115/$ - see front matter © 2008 Elsevier B.V. All rights reserved.
doi:10.1016/j.jnucmat.2008.12.032

In the case of UMo/Al fuels, this ion irradiation has been applied to induce an interaction layer. Successful experiments were performed on a sample with ideal geometry (UMo coated with a thin Al layer [12]), then on UMo/Al fuel plates [13,14]. More recently, a set of UMo/Al samples with different compositions (Mo content in the UMo fuel particles, silicon addition to the Al matrix and coating of the particles with an oxide layer) has been irradiated with heavy ions in strictly identical conditions [15,16]. The aim of this study was to identify the most relevant solutions for limiting the growth of the UMo/Al interaction layer. Positive influences of Si and of a UO_2 protective layer around particles have been underlined. With respect to the silicon addition, this result is in full agreement with conclusions of the post irradiation examination (PIE) of IRIS3 and RERTR6 experiments performed afterwards [17]. For the UO_2 protective barrier around UMo particles, the IRIS4 experiment is currently under design to test this concept [17].

This article is focused on the characterization by XRD (X-ray diffraction) of the interaction layer obtained by heavy ion irradiation. This task is particularly challenging because of the heterogeneity of an ion irradiated fuel plate: the interaction surrounding fuel particles has limited thickness (lower than 10 μm) and depth (lower than 6 μm). A strategy including three different measurements using synchrotron radiation has been defined. First, an average data collection with a 300 μm × 1200 μm X-ray beam has been carried out for high angular resolution. Then, two local characterizations using a micro-focused X-ray beam in reflection and transmission modes were required to enhance spatial resolution [18,14]. Two reference fuel plates UMo7/Al and UMo10/Al (for U–7 wt%Mo/Al and U–10 wt%Mo/Al, respectively) have been studied.

In this paper, after having described sample preparation and heavy ion irradiations, details on the XRD data collection are given. Results of the analyses are then discussed and compared to those obtained for in-pile irradiated fuels.

2. Experimental method

Fresh fuels as well as heavy ion irradiated samples were studied at the 'Laboratoire UO_2' in Cadarache (France). Microscopy was performed using a FEG-SEM-Philips XL30 coupled with an Energy Dispersive x-ray Spectrometer (EDS).

2.1. Mini fuel plate processing and characterizations

Details on the fabrication of mini plates, provided by AREVA-CERCA,[1] have been reported elsewhere [16]. Note, that the uranium density in the meat (consisting of UMo particles and of the matrix) was 7 g cm^{-3} and that fissile particles were small (maximum measured diameter was about 45 μm). On fresh fuel, standard examinations carried out by optical microscopy, SEM and laboratory XRD demonstrate the good quality of the mini plates; only very minor fraction of α-U phase was found.

2.2. Heavy ion irradiation

From the miniplates, large (20 mm × 20 mm) but thin samples (0.5 mm) were prepared at the Heinz Maier-Leibnitz laboratory of Garching (Germany). At the 14 MV tandem accelerator of that laboratory, heavy ion irradiations were carried out under high vacuum in a dedicated set-up that enables temperature measurement and control [13]. The irradiated area (4 mm × 4 mm) at the sample surface has been chosen so that it is large compared to the size of a single UMo particle.

Projectiles representative of the ^{235}U fission products were used: ^{127}I ions with energy of 80 MeV. The final ion fluence was 2×10^{17} cm^{-2}; this value has been reached after 4 h of irradiation. The heavy ion flux has been maintained lower than 1.4×10^{13} cm^{-2} s^{-1} so that sample temperature never exceeds 443 K (this value was determined by a probe (PT100) placed at the rear of the sample). This temperature is slightly high but similar to in-pile temperature for research reactors.

In case of normal incidence, calculations using the SRIM2003 code predict that the penetration depth of ^{127}I ions with 80 MeV energy is about 5.0 μm in UMo7 and about 15 μm in Al [19]. Displacement energies for both U and Mo were set to default values, i.e. 25 eV. To enhance the irradiation density near to the surface and thus improve the efficiency of microscopy analyses, the angle between the incident ion beam and the sample surface was fixed at 30°. ^{127}I mean penetration depth was then 2.61 ± 0.02 μm (beneath the sample surface) and the ^{127}I distribution was broadened (1.64 μm full width at half maximum) (cf. Fig. 3(A)).

2.3. Post-irradiation examinations

First observations using optical or electron microscopy just after the irradiation enabled the distinction of the irradiated from the non-irradiated area at the sample surface (cf. Fig. 1). However the irradiated surface appeared damaged by the presence of ripples [20], making an accurate characterization of the UMo/Al interaction layer almost impossible.

In consequence, samples were cut into four equivalent parts:

- The first part has been analyzed by μ-XRD in reflection mode, without any other preparation.
- The second and the third parts have been dedicated to microscopy studies of the irradiated surface and of the cross section, respectively. To observe the irradiated surface, careful polishing using diamond paste had to be performed: ripples have been removed without altering the UMo/Al interaction layer (Fig. 2(A) and (B)).
- The last part has been used for μ-XRD measurements in transmission mode. The rear side of the sample has been machined (front side being the irradiated one) to reduce sample thickness down to a maximum of 30 μm as usually done for preparing samples for transmission electron investigations. This upper limit has been fixed so that only one fissile particle can be hit at the same time by the X-ray beam when performing μ-XRD transmission measurements. With this preparation, thin samples have been prepared without damaging the irradiated volume.

3. Synchrotron X-ray diffraction

Diffraction measurements were performed at the ESRF (European synchrotron radiation facility) in Grenoble (France). To fulfill safety requirements, samples had to be conditioned under kapton tape.

3.1. Characterization of the entire irradiated area

On the D2AM beamline [21], the photon energy was set to 13 keV. Measurements were performed with a fixed X-ray beam incidence angle (10°) on the sample (to be more sensitive to the ^{127}I irradiated volume) (Fig. 4(A)). In these conditions, beam footprint on the sample was 300 μm × 1200 μm leading to a global characterization of the irradiated surface. Diffraction data were

[1] AREVA-CERCA, a subsidiary of AREVA-NP, an AREVA and Siemens Company.

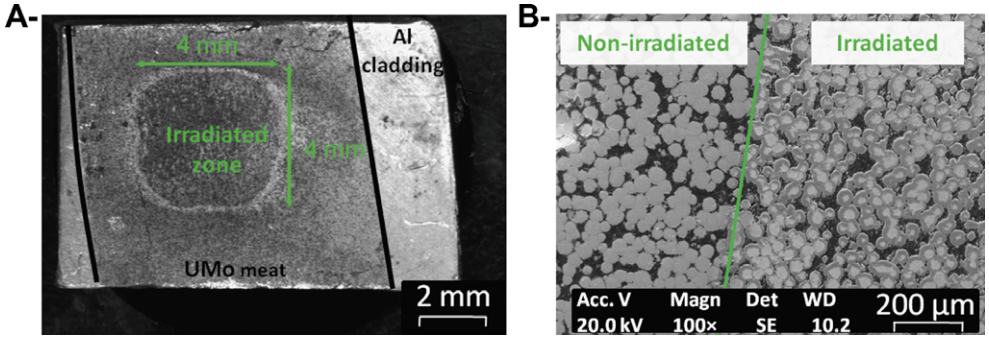

Fig. 1. Comparison between irradiated and un-irradiated area at the UMo10/Al sample surface. In the optical micrograph (A), ripples (cf. Fig. 2) due to the heavy ion irradiation enable the distinction between both zones. In the SEM (secondary electrons) image (B), an interaction layer appears at the periphery of each irradiated particle (ripples have been removed by the sample preparation).

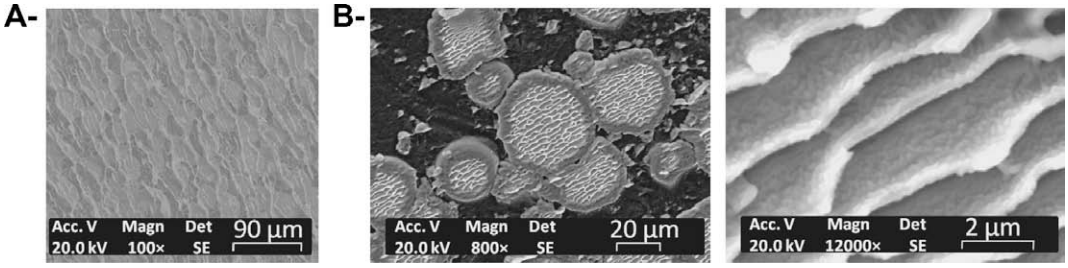

Fig. 2. Two types of ripples that can be observed at the UMo10/Al sample surface in the irradiated area. SEM observations.

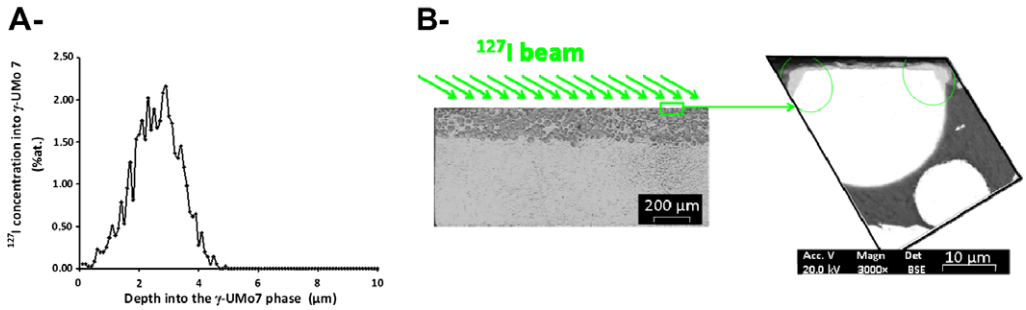

Fig. 3. Comparison between calculated projectile penetration depth into γ-UMo phase (A) and SEM characterization of the UMo/Al interaction thickness (B). Data for the calculation are mentioned in the text and SEM image has been taken in BSE mode on a transversal cross section of the UMo10/Al sample.

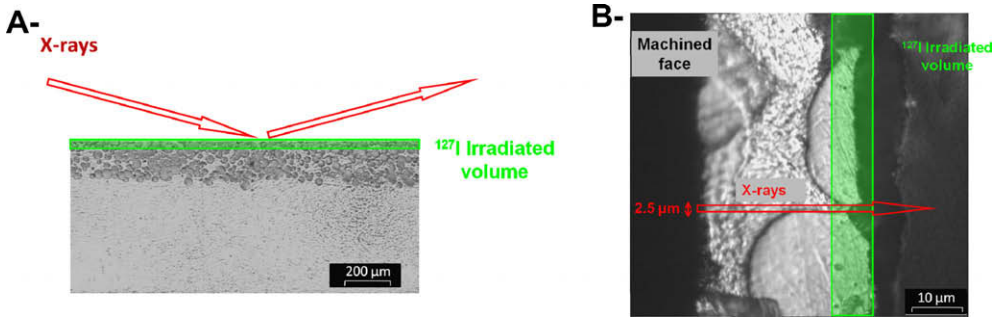

Fig. 4. Schematic representation of X-ray diffraction experiments in reflection (A) and transmission geometry (B).

collected over a wide 2θ angular range (from 10° to 75° with 2600 steps and 5 s counting time per step). Same settings were used to characterize the non-irradiated part of the sample. Both XRD diagrams are compared in Fig. 5.

3.2. Characterization of the interaction layer at the micrometer scale

The excellent spatial resolution of XRD with micro-focused beam should enable isolation of each main component of the

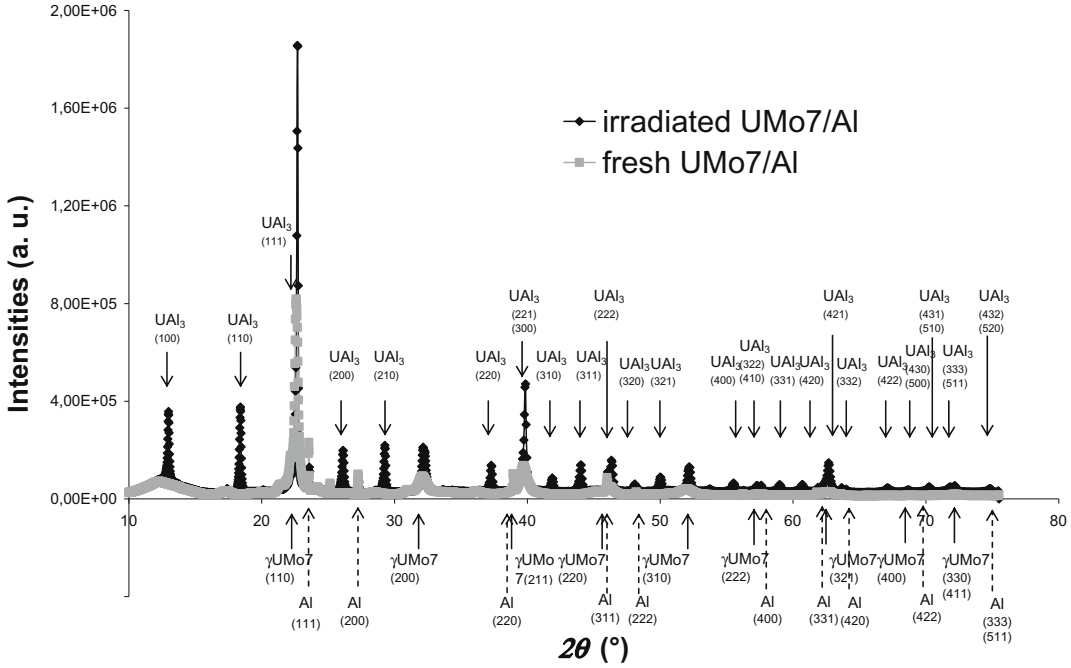

Fig. 5. Comparison of the global XRD patterns collected on the fresh and heavy ion irradiated part of UMo7/Al fuel plate.

sample (Al matrix, fissile particles and interaction layer). Indeed, to be able to assess the presence of ternary $U_xMo_yAl_z$ phases in the interaction layer, as reported in thermally aged UMo/Al samples, the volume probed by X-rays has to be limited to the interaction layer uniquely. The unit cell volumes of these phases are very high and the contribution of theses phases to XRD patterns is weak [18].

Best spatial resolution will be obtained in measurements in transmission mode on thin samples.

However, detailed characterization of the interaction layer should also be performed since some studies report its heterogeneity [13] and since physical phenomena causing the projectile energy loss in the fuel are different with depth.

To control X-ray penetration depth into the fuel plate and, thus, into the interaction layer, data have to be collected in reflection mode (Table 1). Measurements in both geometries have therefore been performed. On the ID-18f beamline [22], photon energy was set to 16 keV and X-ray beam size was about 2.5 μm × 4.0 μm (horizontal and vertical sizes, respectively). The samples prepared for transmission measurement have been placed perpendicular to the X-ray beam and an area covering 77 μm × 117 μm ($H \times V$) has been studied. This corresponds to a mesh of 24 × 27 diffraction images (i.e. 648 images) (Fig. 4(B)).

In reflection mode and to limit the X-ray penetration depth into the sample, the angle between incoming X-ray beam and sample surface has been fixed at 15° [18]. As a consequence, X-ray footprint on the sample was about 2.5 μm × 16 μm. As indicated on the schematic representation of the fuel plate (Fig. 6(A)), a horizontal scan consisting of 370 images has been performed. It has started in the irradiated area and finished in the fresh fuel part of the sample.

In transmission and reflection mode, data acquisition times were set to 5 and 2 s per XRD image, respectively.

Diffraction data were collected using a two-dimensional MAR130 CCD camera with square pixels (size 64.45 μm). These data were reduced to conventional 1D pattern using the FIT2D software package [23].

Table 1
Evolution of X-ray penetration depths in γ-UMo10, UAl_3 and Al.

X-ray energy (keV)	Incident angle on the sample surface (°)	Material thickness probed by X-ray (μm)		
		γ-UMo10	UAl_3	Al
13	10	1	2	28
16	15	1	4	78
16	90	6	17	301

4. Results

Same results have been gathered on heavy ion irradiated UMo7/Al and UMo10/Al specimens.

4.1. SEM on the irradiated surface and fuel plates cross sections

The presence of an interaction layer surrounding each γ-UMo particle has been demonstrated. Their average thickness is slightly influenced by the Mo content of the particles: it equals 7.6 μm in UMo7/Al and 5.6 μm in UMo10/Al.

Moreover cross section observations of the irradiated fuel plate show that an interaction layer has grown down to about 4 μm below the surface (Fig. 3). As expected, this depth is in good agreement with calculated penetration depth of 80 MeV ^{127}I projectile in UMo7 phase.

4.2. Large scale XRD study

XRD global measurements show the presence of the UAl_3 crystal phase after heavy ion irradiation (cf. Fig. 5). Its cell parameter (4.226 Å) appears lower than expected (4.266 Å) [24]. It should be noted that the γ-UMo cell parameter has not been modified by the ^{127}I irradiation. The presence of no other crystal phase could be noticed. However, scattering from the kapton tape packaging makes difficult the identification of amorphous phases.

4.3. XRD using micro-focused X-ray beams (μ-XRD)

This technique enabled the characterization of the interaction layer with an improved accuracy. Thanks to the excellent spatial resolution, interaction compounds could be distinguished from fissile atomized particles.

Results of the global characterization were used to refine the composition of each μ-XRD pattern: only three phases (UAl_3, Al and γ-UMo) were taken into account in the refinement. Indeed, careful analysis of the results does not show the presence of any other crystalline phase.

Semi-quantitative analysis of each collected μ-XRD pattern has been performed automatically using the *FullProf* software package [25]; more details about this data treatment have been given in a previous article [18].

4.3.1. μ-XRD in reflection mode

Results of this refinement procedure are given for only the first 160 μm (inside the irradiated part) and the last 200 μm of the horizontal scan (in the fresh fuel part) for clarity (Fig. 6). In the ^{127}I irradiated part, it is clearly shown that UAl_3 has grown at the expense of the Al phase, this latter having almost disappeared in the 160 first micrometers. Furthermore, UAl_3 weight concentration seems to decrease along the horizontal scan; certain heterogeneity in the ^{127}I beam intensity over the 4 mm × 4 mm could be suspected. Note that some impurities in the UMo particle have been identified: in particular the presence of a very limited proportion of α-U phase has been observed. The first XRD image collected in this scan is shown in Fig. 7. Pure presence of UAl_3 phase can be identified. No $U_xMo_yAl_z$ ternary compound could be found in this sample.

4.3.2. μ-XRD in transmission mode

Location of the UMo particles inside the sample has been obtained via the evaluation of the X-ray attenuation of each part of the sample [18] (Fig. 8). Results of the Rietveld refinements are presented on three weight concentration maps (Fig. 9). As expected, it appears that:

- High Al and γ-UMo concentrations, respectively, correspond to high and low absorption of the sample.
- UAl_3 crystal structure is systematically located at the γ-UMo/Al interface, confirming its presence in the interaction layer.

At the (0,0) coordinates on these maps (Fig. 9), a volume consisting of the interaction layer and the Al matrix situated below has been isolated: only UAl_3 and Al phases have been identified. In this case also, UAl_3 cell parameter equals to 4.226 Å (Section 4.2). When considering the background shape on the derived 1D XRD pattern, the presence of an amorphous phase could not be excluded anymore. Indeed this background is somewhat higher in the 15–23° range (Fig. 10(B)).

4.4. Experimental conclusions

The only crystalline phase which appears due to the heavy ion irradiation is the UAl_3 phase. The in-depth and radial homogeneity of this composition has been shown. However, it was impossible to

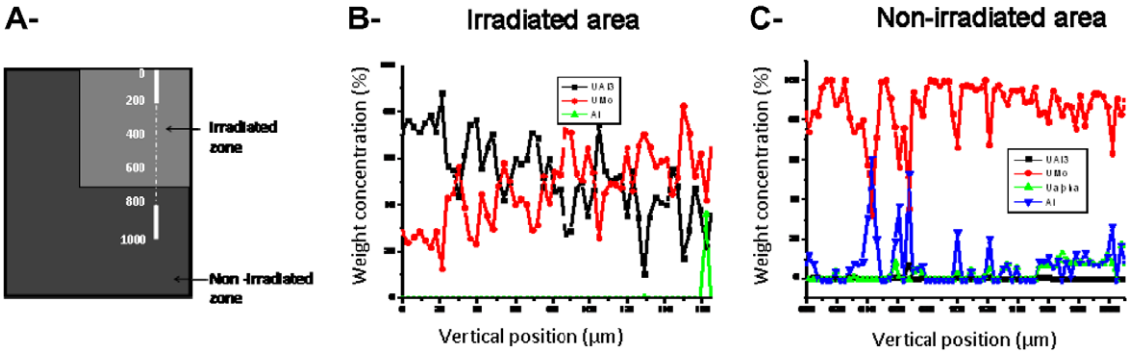

Fig. 6. μ-X-ray diffraction experiments performed in reflection mode on UMo7/Al sample (schematic representation A). Results of the semi-quantitative analysis on selected part of the scan in the irradiated (B) and un-irradiated areas (C).

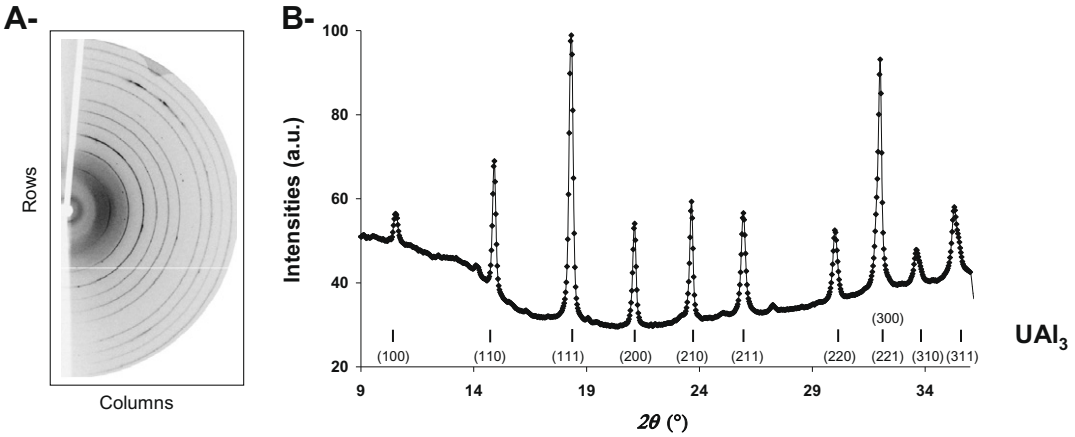

Fig. 7. X-ray diffraction image obtained in reflection mode (A) and the associated 1D diagram (B).

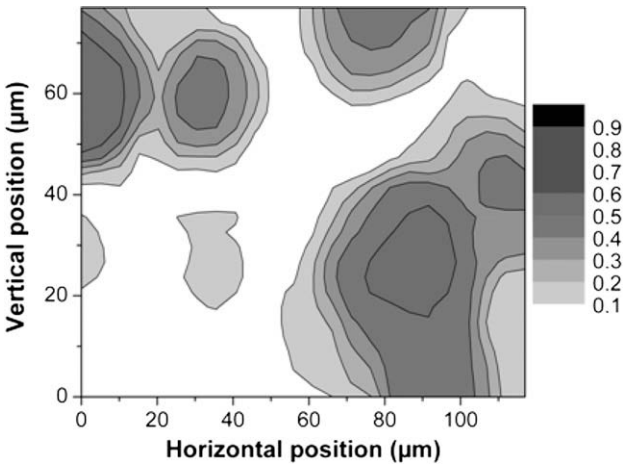

Fig. 8. Evaluation of the X-ray sample attenuation. High values indicate the presence of γ-UMo particles when lower absorptions are associated with Al matrix [18]. However, all fissile particles appearing in this map have not been irradiated since they do not cross the irradiated surface).

conclude whether there was an additional amorphous phase in this interaction layer. A new preparation methodology is under development for addressing this issue [26].

5. Discussion

The results gathered in this study can be compared to those already published on other work using heavy ion irradiation, thermal aging or in-pile irradiation.

It must be stressed that using very similar irradiation conditions, but half the dose, the interaction layer grown on UMo6/Al and UMo10/Al fuel plates were quite close to that found in this study [13]. Indeed, UAl_3 has been identified in both cases as the main component of the interaction layer but other phases have also been found: UAl_4 and UAl_2 in UMo10/Al and only UAl_4 in UMo6/Al.

However, a strong anisotropy of the thickness of the interaction layer grown around the fissile particles as well as its large size (up to 30 μm) are mentioned [13,27] contrary to the results presented here. Since few data on UMo/Al fuel plate heavy ion irradiation can be found in literature, it is very difficult to interpret these differences. More experiments are, thus, required.

5.1. Heavy ion irradiation versus thermal annealing

When comparing the compositions of the interaction layer grown under heavy ion irradiation and during thermal aging, deep differences appear. Indeed at the thermodynamic equilibrium, the presence of UAl_3 phase seems to be always associated with a ternary $U_xMo_yAl_z$ phase and the decomposition of the γ-UMo [7,18]. Under heavy ion irradiation, this XRD study clearly demonstrate that this not the case.

5.2. Heavy ion irradiation versus in-pile irradiation

Even if the presence of amorphous compounds could not be fully assessed in this work, the UMo/Al interaction layer appears mainly crystalline. This result is thus in contradiction with interaction layer composition in fuel plates after in-pile irradiation at similar temperatures (lower than 473 K) [4].

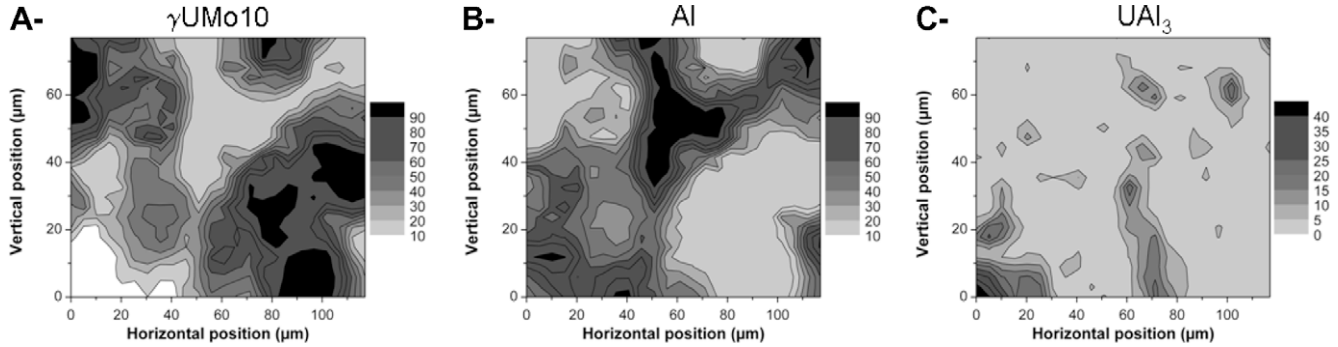

Fig. 9. γ-UMo, Al and UAl_3 weight concentration maps.

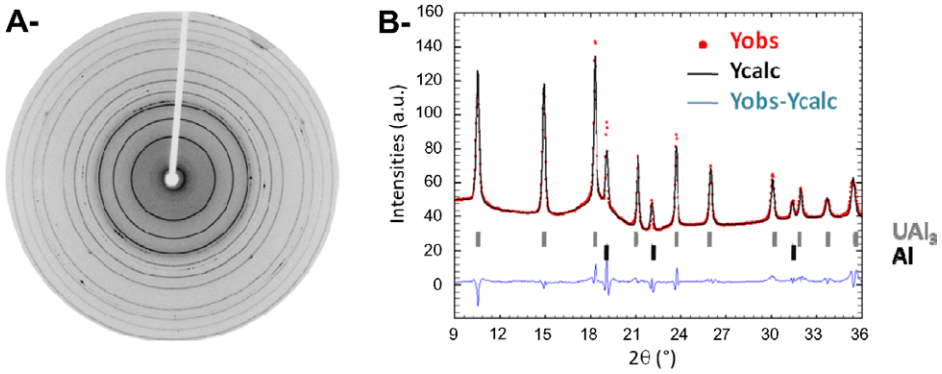

Fig. 10. UMo/Al interaction layer probed by X-ray transmission (2D-image (A) and Rietveld analysis of 1D diffraction pattern). This position is noted (0,0) on the map described in Fig. 9.

The composition of the UMo/Al interaction layer grown under heavy ion irradiation (a high concentration of UAl_3), is close to that found in low burn-up in-pile irradiated fuel rods although the temperature has been maintained quite low during the heavy ion irradiation [5]. Indeed at higher burn-up, fuel rod composition evolves and if UAl_3 still remains the main component, other binary (UAl_2) and ternary (UMo_2Al_{20}) phases appear [6]; their absence from the heavy ion irradiated samples studied here has been underlined.

As a conclusion, a methodological study has to be performed to optimise heavy ion irradiation conditions for better reproducing phenomena occurring in fuel plates during in-pile irradiation under 473 K. With this aim, the influence on the interaction layer composition of the flux, the dose, irradiation temperature and geometry have to be investigated.

6. Conclusion

To characterize accurately the UMo/Al interaction layer grown by heavy ion irradiation, three different measurements were required. This range of complementary measurements (from the millimeter down to the micrometer scale) was used to demonstrate that only one crystalline interaction compound was present (UAl_3). However, the presence of amorphous phases could not be fully assessed.

At this stage, a need for methodological studies has been defined to make this tool more robust to discriminate UMo/Al nuclear fuel plates.

References

[1] M.K. Meyer, G.L. Hofman, S.L. Hayes, C.R. Clark, T.C. Wiencek, R.V. Strain, K.-H. Kim, J. Nucl. Mater. 304 (2002) 221.
[2] F. Huet, J. Noirot, V. Marelle, S. Dubois, P. Boulcourt, P. Sacristan, S. Naury, P. Lemoine, in: Proceedings of the 9th International Meeting on Research Reactor Fuel Management (RRFM), Budapest, Hungary, 2005, p. 88.
[3] A. Leenaers, S. Van den Berghe, E. Koonen, C. Jarousse, F. Huet, M. Trotabas, M. Boyard, S. Guillot, L. Sannen, M. Verwerft, J. Nucl. Mater. 335 (2004) 39.
[4] S. Van den Berghe, W. Van Renterghem, A. Leenaers, J. Nucl. Mater. 375 (2008) 340.
[5] K. Conlon, D. Sears, in: Proceedings of the 10th International Meeting on Research Reactor Fuel Management (RRFM), Sofia, Bulgaria, 2006, p. 104.
[6] K. Conlon, D. Sears, in: Proceedings of the 11th International Meeting on Research Reactor Fuel Management (RRFM), Lyon, France, 2007, p. 140. ISBN: 978-92-95064-03-4.
[7] M. Mirandou, S. Balart, M. Ortiz, M. Granovsky, J. Nucl. Mater. 323 (2003) 29.
[8] J.M. Park, H.J. Ryu, S.J. Oh, D.B. Lee, C.K. Kim, Y.S. Kim, G.L. Hofman, J. Nucl. Mater. 374 (2008) 422.
[9] F. Mazaudier, C. Proye, F. Hodaj, J. Nucl. Mater. 377 (2008) 476.
[10] D.G. Walker, J. Nucl. Mater. 37 (1970) 48.
[11] R.C. Birtcher, J.W. Richardson, M.H. Mueller, J. Nucl. Mater. 244 (1997) 251.
[12] R.C. Birther, P. Baldo, Nucl. Instrum. and Meth. B 242 (2006) 483.
[13] N. Wieschalla, A. Bergmaier, F. Böni, K. Böning, G. Dollinger, R. Grossman, W. Petry, A. Röhrmoser, J. Schneider, J. Nucl. Mater. 357 (2006) 191.
[14] N. Wieschalla, PhD thesis, 2006.
[15] S. Dubois, H. Palancher, F. Mazaudier, P. Martin, C. Sabathier, M. Ripert, P. Lemoine, C. Jarousse, M. Grasse, N. Wieschalla, W. Petry, in: Proceedings of the 28th International Meeting on Reduced Enrichment for Research and Test Reactors, Cap Town, South-Africa, 2006.
[16] H. Palancher, P. Martin, C. Sabathier, S. Dubois, C. Valot, N. Wieschalla, A. Röhrmoser, W. Petry, C. Jarousse, M. Grasse, R. Tucoulou, in: Proceedings of the 10th International Meeting on Research Reactor Fuel Management (RRFM), Sofia, Bulgaria, 2006, p. 99.
[17] M. Ripert, S. Dubois, J. Noirot, P. Boulcourt, P. Lemoine, S. Van Den Berghe, A. Leenears, A. Röhrmoser, W. Petry, C. Jarousse, in: Proceedings of the 12th International Meeting on Research Reactor Fuel Management (RRFM), Hambourg, Germany, 2008.
[18] H. Palancher, P. Martin, V. Nassif, R. Tucoulou, O. Proux, J.-L. Hazemann, O. Tougait, E. Lahéra, F. Mazaudier, C. Valot, S. Dubois, J. Appl. Crystallogr. 40 (2007) 1064.
[19] J.F. Ziegler, J.P. Biersack, SRIM – the Stopping and Range of Ions in Matter, Srim-2003, Computer Code, 2003.
[20] M.D. Hou, S. Klaumünzer, Nucl. Instrum. and Meth. B 209 (2003) 149.
[21] J.-L. Ferrer, J.-P. Simon, J.-F. Bérar, B. Caillot, E. Fanchon, O. Kaïkati, S. Arnaud, M. Guidotti, M. Pirocchi, M. Roth, J. Synchrotron Rad. 5 (1998) 1346.
[22] A. Somogyi, M. Drakopoulos, L. Vincze, B. Vekemans, C. Camerani, K. Janssens, A. Snigirev, A. Adams, X-ray Spectrom. 31 (2001) 242.
[23] H. Hammersley, 1999, <www.esrf.fr/computing/scientific/fit2d>.
[24] J. Faber, G.H. Lander, Acta Crystallogr. A37 (1981) 558.
[25] J. Rodriguez-Carvajal, *FullProf*, version 3.40, LLB, CEA/Saclay, France, 1990, <http://www.llb.cea.fr/fullweb/poudres.htm>.
[26] H. Palancher, P. Martin, E. Welcomme, F. Mazaudier, S. Dubois, C. Valot, R. Tucoulou, P. Lemoine, in: Proceedings of the 30th International Meeting on Reduced Enrichment for Research and Test Reactors, Washington, United States, 2008.
[27] R. Jungwirth, W. Petry, W. Schmid, L. Beck, in: Proceedings of the 12th International Meeting on Research Reactor Fuel Management, Hambourg, Germany, 2008.